Breakdown Wave, Shock Wave, and Radiation Wave in Laser Created Plasmas

P. VEYRIE* AND F. FLOUX†
Commissariat à l'Energie Atomique, Paris, France

The various phenomena occurring during the growth of laser generated plasmas are both theoretically and experimentally presented. The experimental results obtained with short and long laser pulses, and short and long focal lengths are described. Their interpretation is based on three different models, depending on experimental condition. The existence of an ionization threshold implies the possibility of a breakdown wave, especially in the case of short pulses, or the formation of a radiation supported shock wave. For experiment with high-density targets, the opacity may be so high that the thermal radiation conductivity is the principal reason for propagation of ionization and heating.

Nomenclature

a = thermal sound velocity
c = speed of light
D = velocity of waves
E_0 = energy of radiation
F = free diffusion coefficient of electrons
h = Planck constant
I = flux density of laser light
K = absorption coefficient
k = Boltzmann constant
n = number density for unit volume, cm^{-3}
P = laser beam power
p = pressure
r,x = positions
T = absolute temperature
t = time
u = material velocity
Z = atomic number
β = recombination coefficient
ν = frequency of creation of electron
χ = ionization potential
Ω = geometrical parameter (generally a solid angle)
τ = delay to ionization
ρ = mass density
γ = polytropic coefficient
ΔE_0 = band width of radiation
λ = mean free path

Subscripts

0 = initial or neutral
B = related to Bremstrahlung
C = related to breakdown
E = expansion fan
e = associated to electrons
i = related to ionization by collisions
P = Planck
R = radiation wave
RO = Rosseland
S = shock wave
t = related to threshold or direct ionization

Presented as Paper 68-678 at the AIAA Fluid and Plasma Dynamics Conference, Los Angeles, Calif., June 24–26, 1968; submitted August 5, 1968; revision received January 20, 1970. The works presented here are the fruit of the collective effort of a group, and each member of the team took his part in the results. We are especially indebted to J. L. Bobin, C. Fauquignon, and R. Gasnier for their assistance in theoretical models.

* Docteur des Sciences.
† Ingenieur.

I. Introduction

SINCE first observed in 1963[1,2] the creation of a plasma by a giant pulse laser beam focused within a gas has been extensively investigated as a technique for heating matter to high temperature. Various aspects of the problem have been distinguished and the literature offers studies about gas preionization,[3,4] ionization cascade,[5,6] hydrodynamic behavior,[7–9] and breakdown wave phenomenon.[10]

Recently, experiments on ionization and breakdown within transparent solid deuterium ice[11] suggest that the results obtained with gases may be extended to the higher target densities associated with such solid materials.

In this paper, we shall review some typical situations for experiments within gases and transparent solids before developing different interpretations based on hydrodynamic behavior or radiation transfer.

II. Experimental Results

Laser Optics

All the experiments have been carried on with C.G.E. neodymium glass laser. All arrangements have been derived from the same basic system; a rotating prism Q switched oscillator followed by a cascade of amplifiers. Rods are from neodymium glass. Output diameter of last stage is 32 mm. The maximum energy delivered was 30 joules within a 30 nsec pulse. In every case but those specified, we used an f/1 40 mm focal length lens. This lens is a specially devised spheroelliptical one completely corrected for spherical aberrations.[12]

In the first experiments, the optical quality of the laser beam was not perfect due to astigmatism. This has been extensively studied in Ref. 13.

The association of the beam with the spheroelliptical "perfect" lens gave a minimum focal spot size of 200 μm diameter. The results described in Figs. 1, 5, and 7 were obtained from this association. In Fig. 4 a modified arrangement was used to try to improve beam quality and raise the pulse to 60 joule. The resulting pulse width was the same but now we get a focal spot of 40 μm with the same "perfect" lens.

To get shorter pulses the laser was modified by inserting a KDP Pockels and glass prism between the oscillator and the first amplifier. The result was a 5 nsec, 10 joule, fast rise time pulse. The optical quality and thus spot size remained unchanged (Fig. 3). To test the importance of the

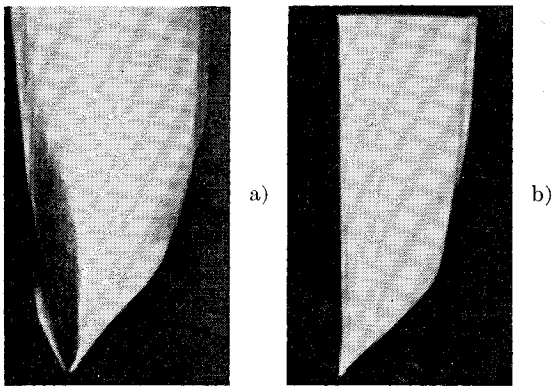

Fig. 1 Shock waves in gases (30 nsec laser pulse). The laser beam is coming from the right. The sweep duration of the streak camera is 200 nsec, focal length = 40 mm. a) Deuterium, p = 3 atm. b) Air, p = 1 atm.

optical quality (Fig. 2) some experiments were done with an ordinary commercial biconvex lens, f = 100 mm.

Studying the radiation distribution in the neighborhood of the supposed focus, we found several maxima of light intensity along the beam axis, probably due to a combination of spherical aberration and diffraction.

Results of Interaction

Experimental evidences with which we are dealing are based on Space Technology Laboratory (STL) streak camera pictures which give the time history and the main features of the plasma expansion. In Fig. 1, the plasma expansion as is obtained with sharp focusing, 30 nsec pulse, is reported. The velocity of the front is about 6×10^6 cm/sec for deuterium gas and 1.2×10^7 cm/sec for air. As shall be later seen, these velocities are readily interpreted on the basis of a radiation supported shock wave.

In Fig. 2 we present some of the results we got with poor focusing of the same beam. The various breakdowns are approximately initiated where the previously mentioned peaks of light intensity are located. The coincidence is not rigorous as the effect is a complex one. At the nearest maximum from the lens, a radiation-supported shock wave starts, which may or may not screen the breakdown at the next maximum. Important factors are then, the geometrical distribution of light, the velocity of the shock, and the pressure of the gas. The purpose of the photograph is to show the great importance of sharp focusing.

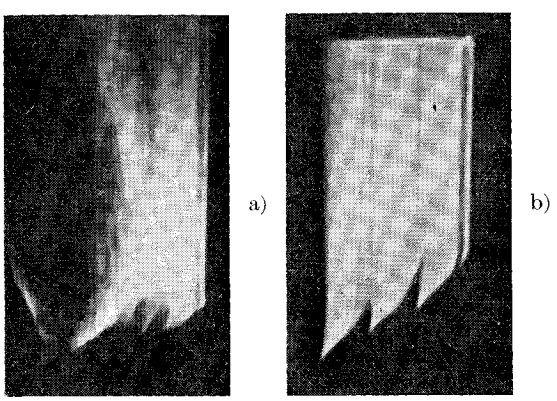

a) Deuterium, p = 3 atm. **b) Air, p = 1 mat.**

Fig. 2 Breakdown waves in gases (30 nsec laser pulse). The laser beam is coming from the right. Sweep duration is the same as Fig. 1. On each picture, one may distinguish multiple breakdown during the plasma expansion, focal length 40 mm.

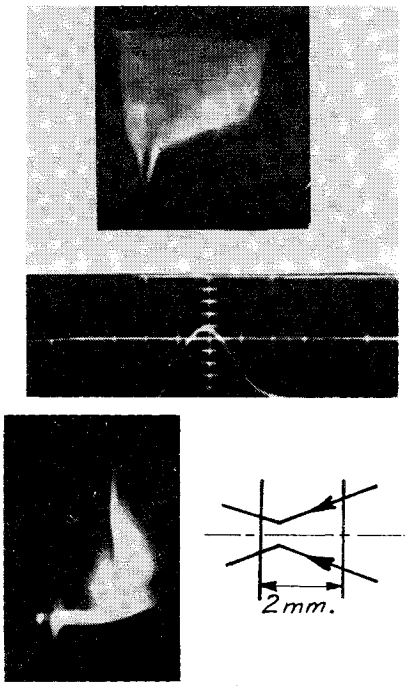

a) Deuterium gas, p = 1.8 atm (time scale: 5 nsec/div)

b) Deuterium ice

Fig. 3 Breakdown waves with 5 nsec laser pulse. The gas and solid cases have been represented on the same figure. The 5 nsec half width, 2×10^9 w laser pulse is coming from the right and oscillogram of this pulse has been reported on the left side. The sweep rate of streak pictures is 1 nsec/mm, in both cases, a 40 mm focal length, f/1 focusing lens has been used.

Figure 3 illustrates the breakdown with short pulses. Such velocities close to 10^8 cm/sec cannot be explained by a hydrodynamic mechanism. We shall present an interpretation in the next section.

At last in Fig. 4 streak camera pictures obtained when focusing the 30 nsec 60 joule laser beam on a solid deuterium ice[11] are reported. Figure 4a was taken when focusing in the center of the 2 mm^2 square section of ice. We notice that multiple breakdown propagates towards the free surface until the luminous front merges. This multiple breakdown is due to the fact that the sharp focused beam is distorted by the poor quality dioptra separating the deuterium ice from air. Then, the ionized zone travels back into the ice and at the same time, plasma expansion into vacuum occurs by focusing on the surface. Figure 4b phenomena show only evidence of inwards and outwards propagation that we shall study in part V.

During this experiment, it has been possible to get plasma electron temperature by means of x-rays continuous emission measurements. Assuming that the recorded soft x-rays are due to bremstrahlung emission, correlations‡ between measured electron temperature and inwards luminous front velocities have been achieved (Table 1).

III. Threshold-Ionization and Breakdown Wave

Many experimental and theoretical works suggest that when the flux density of laser light exceeds a threshold value I_t, there is a direct ionization of the irradiated matter and subsequent creation of free electrons. There are as many mechanisms described for that ionization as there are people involved in that research, but the result can always be written with the same expression, which is a frequency designated as ν_t, for creating free electrons out of the neutral matter that ceases to be null.

‡ We are not yet able to determine the spatial origin of x-rays.

Table 1 Experimental electronic temperature T and recorded front velocities V_r (values are given in CGS units)

T, °K	V, cm/sec
10^6	0.9×10^6
1.3×10^6	1.4×10^6
1.8×10^6	1.6×10^6

With the preceding statement it is possible to write the equations for electronic population and energy

$$\partial n_e/\partial t = \nu_t(n_0 - n_e) + \nu_i n_e + F\nabla^2 n_e - \beta n_e^2$$

$$d/dt[n_e(\tfrac{3}{2}kT + \chi)] = K_t I(t) + K_B I(t)$$

where ν_i = ionization frequency by collisions of electrons on neutral atoms, and F = the diffusion coefficient of electrons out of the reaction zone; hence $F\nabla^2 n_e$ represents the loss of electrons by diffusion. βn_e^2 = the loss of electrons by recombination, K_t = an absorption coefficient related to direct ionization, K_B = the absorption coefficient of light by bremstrahlung of electrons in the fields of ions or inside the atomic shells, n_0 = the neutral density, and χ = the ionization potential. This system is general and may be used for various experimental conditions. We solved it using the values of our first series of experiments; laser pulse 30 joule, 30 nsec, focused to a 200 μm diam spot.

To simplify diffusion calculations, the focal volume was taken to be a cube of 2×10^{-6} cm^3. Pressures were varied from 300–3000 torr of deuterium. The following assumptions were made: ν_t is zero for $I < I_t$, ν_t reaches a value for $I \geq I_t$ which will be adjusted from experimental results, the recombination term is negligible (computations show that this assumption is valid in our pressure range), and the absorption coefficient is the free-free absorption one; the electron neutral coefficient is negligible for the case studied here of $Z = 1$ and our pressure range.

The boundary condition was that of a measurable absorption of light (exceeding the experimental accuracy of 5%) that corresponds to the time of appearance of a luminous plasma. With origin of times when $I = I_t$, this time will be denoted τ and called ionization duration. Its physical meaning is the time necessary for ionization to develop sufficiently for a noticeable absorption of radiation and a subsequent luminosity to be obtained. After time τ things will proceed in a different way which we shall consider later.

Experimental values of τ are presented in Fig. 5 with their incertainty bar. They are compared with the results of the computation previously described. These experimental values were deduced from measurements of the laser power transmitted through the plasma and were extensively described in Ref. 15.

With a sufficiently high-brightness laser, the flux density may increase after having reached the level I_t. Consequently the threshold conditions may be met in larger cross sections of the conic laser beam. Let some electrons be created at a distance r_c from the focus. At time τ afterwards, the breakdown will occur at the distance r_c. Thus we may write the condition

$$P(t - \tau)/\Omega r_c^2 = I_t$$

which means that if we observe a breakdown on r_c at time t with power $P(t)$, threshold will be reached in this place, τ nsec before.

Ω is a geometrical coefficient. If the focused beam is a uniform one, Ω is the beam solid angle. If not, Ω should be a parameter that relates the power $P(t)$ to the flux density at r_c.

The preceding expression shows that the ionization may propagate towards the focusing lens following what Raizer[10] calls a breakdown wave. The position of that breakdown

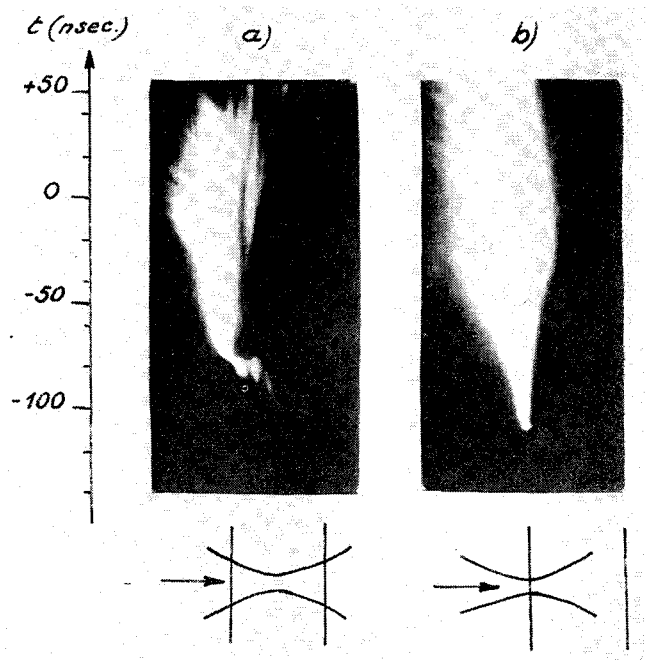

Fig. 4 Deuterium ice experiment (30 nsec laser pulse). Streak camera pictures of the solid deuterium case have been reported for two focusing conditions a and b. The laser is coming from the left. The inwards luminous front propagation is interpreted as a shock wave. On the other hand, one may find multiple breakdown phenomena in the first stage of case a between 100 and 90 nsec, when the plasma is travelling inside the ice. Time zero has been taken for the laser peak value.

wave is given by

$$r_c = [P(t - \tau)/\Omega I_t]^{1/2}$$

If the plasma is sufficiently transparent, there can be also a breakdown wave in the opposite direction, given by

$$r_c' = [T(t - \tau)/\Omega I_t]^{1/2}$$

where T is the transmitted power.

If other mechanisms (shock waves) are not masking the breakdown wave, it will be and has been experimentally observed (Figs. 2 and 3). The breakdown wave depends on Ω.

If the focal length is increased, Ω is decreased; hence, the velocity dr_c/dt of the breakdown wave should be increased. In fact the phenomenon is complicated by on-axis diffraction that gives extremes of flux density where start successive breakdowns. This explanation holds for poor focusing as on pictures presented in Fig. 2. The breakdown wave velocity depends also on $dP(t)/dt$, that is on the rise time of the pulse.

With nanosecond pulses we get very fast wave. In Fig. 6 are plotted the streak-camera-observed position of the luminous front compared with computed values of r_c and r_c'.

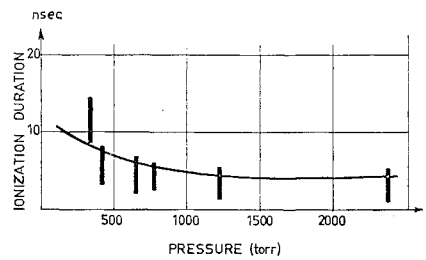

Fig. 5 Ionization duration $\lambda_t = 5 \times 10^6$ vs gas pressure. The experimental observed values have been reported with experimental uncertainties (vertical lines).

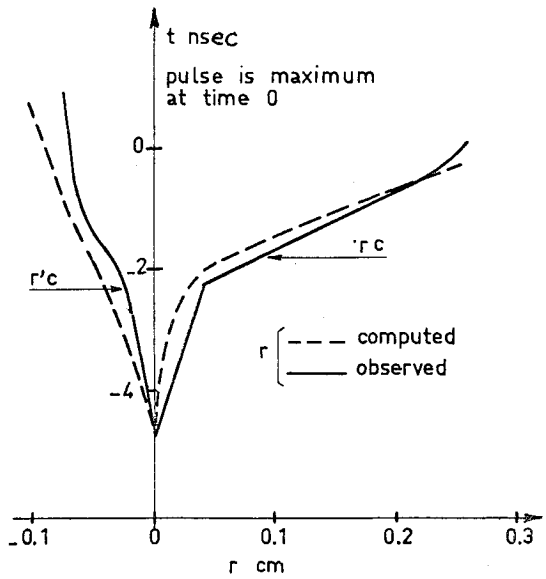

Fig. 6 Breakdown wave in gases. 2 nsec laser pulse has been used on the graph, the laser beam is coming from the right. The position $r = 0$ corresponds to the focal area of the focusing lens (spheroelliptical $f/1$ 40 mm focal length).

There is a good agreement for r_c in the high velocity region (other parts are explained by hydrodynamics).

There is disagreement for r_c', but measurement of transmitted power $T(t)$ is not quite accurate when short pulses are involved. Peculiarly, time history of incident light, transmitted light, and streak pictures are very difficult to associate with respect to each other.

IV. Hydrodynamics

When the breakdown wave can be assumed slower than the shock wave, the plasma created at time τ will follow a hydrodynamic evolution. These conditions are met when the laser pulse is not too fast and when we obtain a sharp focusing.

Thus, at time τ, after initiation, we get initial conditions of temperature and density in the focal volume. We may compute the hydrodynamic expansion in both directions towards the lens and backwards. A shock wave is created and radiation supported in the conical laser beam. Because of the nonstationary character of the problem a numerical solution was sought.

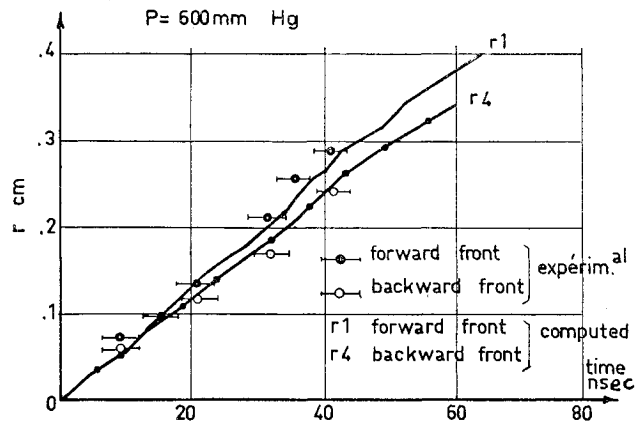

Fig. 7 Plasma dimensions vs time (30 nsec laser pulse). r is the dimension of plasma along the laser beam axis (see Fig. 6). In this graph, time zero is taken when the luminous plasma appears on streak picture. The laser peak value is reached for about 40 nsec.

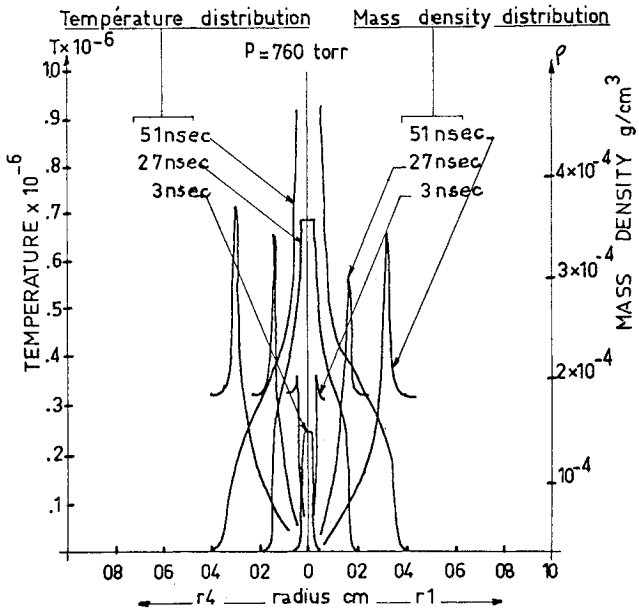

Fig. 8 Shock structure. Computed profiles of mass density and electronic temperature of the plasma have been reported for different times during the laser pulse. Time zero is the same as in Fig. 7. The laser beam is coming from the right. The origin of the process ($r = 0$) is the focal area.

We got satisfactory results by resolving the set of hydrodynamic continuity equations together with radiation transfer ones.

In Fig. 7 we have plotted the computed results concerning both shock waves. One propagating towards the lens, the other in the opposite direction. The example here is taken at a pressure of 600 torr of deuterium with 30 nsec 30 joule laser. Experimental results are represented with their incertainty bar.

From computation we also deduce temperature and density distribution across the shock as a function of the radius (Fig. 8). The temperature is maximum at the focus ($r = 0$) where density has a minimum with very low value. We can follow the mechanism of heating in that figure. The leading shock discontinuity causes sufficient ionization and temperature so that the absorption of light may be important. This absorption heats the fluid to a maximum temperature in the center where, because of the radial expansion, mass has been nearly completely evacuated. Hence from the discussion presented in part III and IV, we find that two eventualities may occur for breakdown of gases; a breakdown wave for poor focusing or very fast rising pulses, and a radiation supported shock wave for sharp focusing and not too fast a pulse (ten nsec or more rise time). We shall now turn to solid deuterium targets to see how these conclusions are modified.

V. Hydrodynamic Model for Deuterium Ice Experiment

The experimental results concerning solid deuterium can be summarized in the following way: 1) we have found that somewhere in the plasma there was a temperature of more than 10^6° depending on the experimental condition,[14] and 2) we have measured the velocity of the luminous front propagation inside the plasma.[11] Furthermore we can assume that laser radiation is stopped when the plasma frequency is equal to laser frequency.

We then compute the following plane one-dimensional model. A similar approach was derived by Caruso et al.[16] in his general principle. A shock wave is propagating inside the solid ice with a constant velocity D_S. The radiation is

Table 2 Experimental front velocities Vexp, compared with calculated ones, D_R and D_s, for different values of electronic temperature T

T, °K	D_R, cm/sec	D_s, cm/sec	V_{exp}, cm/sec
1×10^6	1.2×10^6	1.4×10^6	0.8×10^6[a]
1.3×10^6	1.4×10^6	1.6×10^6	1.4×10^6
1.8×10^6	1.6×10^6	2×10^6	1.6×10^6

[a] This figure is uncertain because of the small velocity.

incident on the vacuum boundary of the shocked materials and propagates with a constant velocity D_R, smaller than D_S. Behind this penetration of radiation, there is free expansion of the plasma into the vacuum. We assume that the plasma is isothermal in the region crossed by the radiation. The adiabatic cooling is supposed to be compensated for by some absorption. As the plasma frequency cut-off operates as a wall preventing the absorption of radiation further than the thin layer of the skin effect, we may suppose that velocity D_R equals velocity u_S behind the shock discontinuity. The theory of isothermal free expansion wave, designated here by subscript E, implies that we introduce a constant,

$$a = (p_E/\rho_E)^{1/2} \tag{1}$$

and thus find that along trajectories described by

$$x = (u_E + a)t \tag{2}$$

the density decreases exponentially

$$\rho_E = \rho_R \exp[(u - u_R)/a] \tag{3}$$

ρ_R and u_R are densities and velocities at the point R reached by the radiation.

At this point we have no reason to find continuity in density and velocities. In fact the strong absorption region has some thickness. There we get a strong variation in temperature, density, and velocities of the fluid, but we overlook this and treat it as a discontinuity that obeys the following relations:

$$\rho_R(D_R - u_R) = \rho_S(D_R - u_R) \tag{4}$$

$$P_S = 2\rho_R a^2 \tag{5}$$

Equation (4) shows that because $D_R - u_S$ is negligibly small, ρ_R will be very small; another way of expressing the aforementioned discontinuity.

The shock wave follows the classical expression that one may deduce from Rankine-Hugoniot equations

$$\rho_S = \rho_0(\gamma + 1/\gamma - 1) \tag{6}$$

$$P_S = \tfrac{1}{2}(\gamma + 1)\rho_0 u_S^2 \tag{7}$$

$$D_S = \tfrac{1}{2}(\gamma + 1)u_S \tag{8}$$

where γ is the polytropic coefficient of the shocked region (high density and low temperature). Ignoring the exact value of temperature in this region, we have chosen γ as equal to the diatomic $\frac{7}{5}$ value.

The energy relationship corresponding to expansion wave and radiation discontinuity has not been written for the simple reason that we do not know how to solve it without a computer, which would in fact solve the problem in a different way.

Thus the system of equations written previously is not sufficient. Therefore we have to get two more parameters. One of them is the temperature given by the experiment and the second one is ρ_R imposed by cut-off consideration. From T we deduce a [Eq. (1)], from P_R we deduce P_S [Eq. (5)], and similarly u_8 [Eq. (7)], D_S [Eq. (8)], and D_R.

In Table 2 we have reported experimental values for T and front velocity, Vexp, compared to computed ones out of T and D_R.

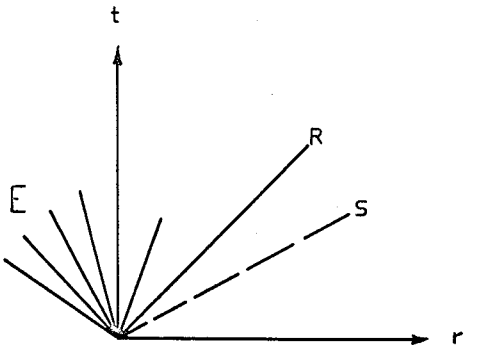

Fig. 9 Hydrodynamic behavior of the plasma in the deuterium ice experiment. In the (r, t) diagram, one may assume the shock wave S and the deflagration front R followed by a rarefaction fan. Origin of the process is taken at the free surface of the ice.

The observed luminous front should be the radiation front rather than the shock front. In fact at shock velocities of the order of 10^6 cm/sec, the temperature of solid deuterium remains very low and ionization is not important. Thus the shock front may not be sufficiently luminous to be recorded.

Our interpretation of the experimental pictures is given in Figs. 9 and 10.

To conclude, a very simplified model can account for part of the experimental results. We have to do this one in order to see if our assumptions are reasonable. In other words, the resolution of the problem with a computer will be the answer to this question.

VI. Radiation Wave

We are to consider another kind of explanation for the observed luminous front; that is a mechanism of radiative heat conduction. We shall restrict ourselves to the main features of such a process and provide some remarks about orders of magnitude that may be involved in our experiment.

Let us consider an optically thin and high temperature plasma layer bounded by a cold and poorly ionized medium. A part of the thermal radiation may be strongly absorbed by the colder layers while the high temperature layer is transparent to its own radiation. In deuterium ice the mean free path of thermal photons lies between 10^{-5} and 10^2 cm for temperature of 10^5 °K up to 10^7 °K. Thus each layer of cold deuterium may be heated by the thermal radiation emitted by the preceding one. This heating is governed by radiative heat conduction which strongly depends on temperature resulting in a nonlinear heat conduction equation. Zel'dovich and Raizer[17] have described such a mechanism and given the

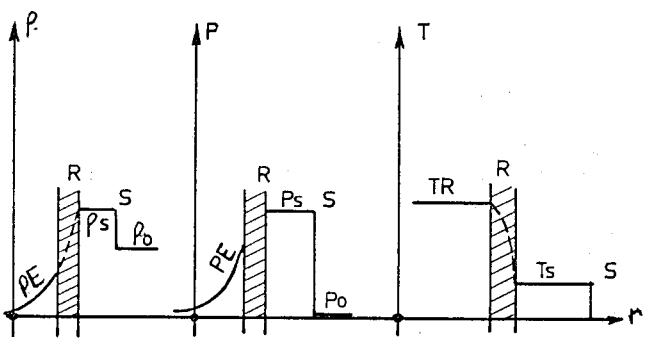

Fig. 10 Mass density, pressure, and temperature profiles inferred by the hydrodynamic behavior represented in Fig. 9. The subscript S is used for the shocked region, R for the deflagration front, and E for the rarefaction fan (plasma into expansion).

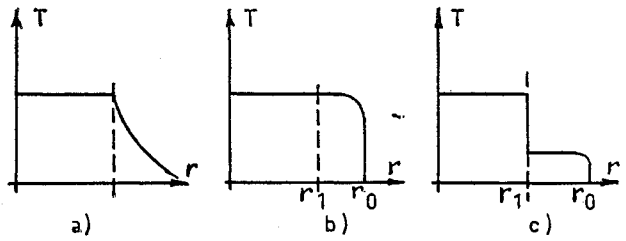

Fig. 11 Theoretical temperature profiles vs distance in three different heat conduction mechanisms: a) for classical heat conduction; b) for nonlinear heat conduction with radiation into equilibrium; and c) nonlinear heat conduction with radiation out of equilibrium.

temperature profiles to be reached in the cases shown in Fig. 11.

The difference between Fig. 11b and Fig. 11c takes into account the heated region transparency and its own radiation. We shall notice that in the case where $x_0 - x_1$ is small compared with outer dimensions of the system, then the colder layers may reach a temperature closer to that of the heated region.

In Fig. 11c, one may reach a satisfactory qualitative picture by the following simple argument. Suppose that between the x and x_0 planes only the radiation enclosed within a narrow band ΔE_0 near energy E_0 is actually absorbed by the cold layers. Then one may readily show that energy conservation reads

$$2E_0^3\Delta E_0/h^3c^2 \exp(E_0/kT - 1) = (\tfrac{3}{2}n_0kT + \chi)d\chi/d\tau \quad (9)$$

T is the temperature of the black body spectrum emitted in the x plane, towards the positive x direction, n_0 is the partical density in the cold medium, χ is the ionization energy density, and dx/dt is the velocity of the front x_0 with respect to x_1.

Since in the temperature range involved in our experiment, χ is either negligible or of the order of kT per ion, Eq. (1) reduces to

$$d\chi/d\tau = A/T(\exp B/T - 1) \quad (10)$$

Thus, if the driving temperature T is constant, dx/dt is also a constant. If the driving temperature is $T = T_0 \exp\alpha t$ then $dx/dt = A' \exp(-\alpha t)/\exp B' \exp(-\alpha t)$ and reaches a constant value A'/B' for $t \to +\infty$.

A more accurate theory will involve the diffusion approximation. Satisfactory results have been obtained by R.E. Marshak[18] in Fig. 11b with a driving temperature given by Eq. (3).

This radiative mechanism is strongly dependent on two mean free paths which are: 1) λP (Planck mean free path) which characterizes the blackening of the emitting layer, 2) λRO (Rosseland averaged m.f.p.) which gives the thickness of the radiative wave.

In the Table 3, we have reported λ_P and λ_{RO} values for different temperatures and solid deuterium ($\rho_0 = 0.17$) (including scattering). From these values, one may conclude that radiative heat conduction may be taken into account in our experiment, in the 10^6 °K range. Moreover we notice that the cold medium density is greater than ρ_0 as a result of the shock wave and that the inverse bremsstrahlung absorption of electron with neutral atoms have to be included in the calculations of λ_R and λ_B.

These two corrections may reduce appreciably the values of these characteristic lengths. But exact calculations have not yet been performed.

This tentative explanation is only a prospective one. We need more computations. In fact hydrodynamic model and radiative model for solid deuterium interaction are not exclusive of each other. We may readily imagine that the penetration of radiation inside the deuterium ice will be accompanied by re-emission of equilibrium light that might be absorbed in vicinity layers, thus increasing the strength of the shock. But computation of such a complicated process is rather difficult.

Table 3 Calculated values of λ_P and λ_{RO} vs electronic temperature T

T	10^5°K	10^6°K	10^7°K
λP, cm	10^{-5}	3×10^{-2}	72
λRO, cm	6×10^{-4}	2	27

VII. Conclusion

We shall conclude this review of phenomena by some considerations of the various situations that may occur during the plasma growth.

At first, one may identify each process by comparing the fluid velocity with that of radiative absorption whenever the radiation comes from laser (breakdown wave) or from heat conduction. For example, in the breakdown case, the laser absorption zone moves faster than the fluid. However, for the case of interaction with solids, we have described a process where the shock velocity travels faster than laser radiation penetration.

The two main parameters governing the nature of the process involved in the expansion are the laser power and the rise time of the pulse connected with the focusing characteristics. For sharp and good focusing lens, we have mainly observed hydrodynamic behavior when long rise time laser pulses are used, and breakdown wave with shorter rise time pulses.

Density of the target plays a role also. For solid transparent targets, cascade duration τ is negligible, thus breakdown is very fast. In the first nanoseconds of the interaction, the breakdown wave is predominant. In fact the situation is complicated by the poor optical quality of the ice with the consequence of multiple breakdown. As interaction proceeds, the various mechanisms might successively occur. An example for that is found in Fig. 3 where we distinguish a shock wave in the first nsec followed by a breakdown wave. Another example in Fig. 4 where multiple breakdown within the ice is followed by a breakdown wave.

References

[1] Maker, P. D., Terhune, R. W., and Savage, C. M., "Optical Third Harmonic Generation," *Proceedings of the 3rd International Conference on Quantum Electronics Paris*, Dunod, Paris, 1964, pp. 1559–1576.

[2] Meyerand, R. G. and Haught, A. F., "Gas Breakdown at Optical Frequencies," *Proceedings of the 6th International Conference on Ionization Phenomena in Gases*, SERMA, Paris, 1963, pp. 479–490.

[3] Berry, M. et al., "Etude Experimentale et Théorique du Claquage de l'Air sous l'Action d'un Faisceau Laser," *Compte Rendus à l'Academi des Sciences de Paris*, Vol. 259, Oct. 1964, pp. 2401–2403.

[4] Nelson, P., "Calcul de l'Onde de Grandeur des Processus Multiphoniques," *Compte Rendus à l'Academi des Sciences de Paris*, Vols. 251–259, Oct. 1964.

[5] Phelps, A. V., "Theory of Growth of Ionization during Laser Breakdown," *Proceedings of the Physics of Quantum Electronics Conference*, McGraw-Hill, New York, 1966, pp. 538–547.

[6] Zel'dovich, Y. B. and Raizer, Y. P., "Cascade Ionization of a Gas by a Light Pulse," *Soviet Physics JETP*, Vol. 20, No. 3, March 1965, pp. 772–780.

[7] Ramsden, S. A. and Savic, P., "A Radiative Detonation Model for the Development of a Laser Induced Spark in Air," *Nature*, Vol. 203, No. 4591, Sept. 1964, pp. 1217–1219.

[8] Floux, F. and Veyrie, P., "Etude Expérimentale des Plasmas Créés par Focalisation d'un Faisceau Laser dans l'Air," *Compte Rendus à l'Academie des Sciences de Paris*, Vol. 261, Nov. 1965, pp. 3771–3773.

[9] Champetier, J. L., "Interprétation Théorique de l'Évolution du Plasma Créé par Focalisation d'un Faisceau Laser dans l'Air," *Compte Rendus à l'Academie des Sciences de Paris*, Vol. 261, Nov. 1965, pp. 3954–3957.

[10] Raizer, Y., "Heating of a Gas by a Powerful Light Pulse," *Soviet Physics JETP*, Vol. 21, No. 5, Nov. 1965, p. 1009.

[11] Colin, C. et al., "Laser Produced Plasma from Solid Deuterium Targets," *Journal of Applied Physics*, Vol. 39, No. 7, June 1968, pp. 2991–2993.

[12] Champetier, J. L. et al., "Utilisation de Lentilles Asphériques pour l'Obtention d'Éclairements Élevés," *Compte Rendus à l'Academie des Sciences de Paris*, Vol. 266, March 1968, pp. 838–841.

[13] de Metz, J., Terneaud, A., and Veyrié, P., "Etude Optique du Faisceau Émis par un Laser de Grande Intensité," *Applied Optics*, Vol. 5, No. 5, May 1966, pp. 819–822.

[14] Bobin, H. L. et al., "X Rays from a Laser Created Plasma," *Physics Letters*, Vol. 28 A, No. 6, 1968, pp. 398–399.

[15] Veyrie, P., "Contribution à l'Etude de l'Ionisation et du Chauffage des Gaz par le Rayonnement d'un Laser Déclenché—Résultats Experimentaux," *Le Journal de Physique*, Vol. 29, Jan. 1968, pp. 33–41.

[16] Caruso, A., Bertotti, B., and Guiponni, P., "Ionization and Heating of Solid Materials by Means of a Laser Pulse," Il Nuovo Cimento, Vol. XLV, No. 2, Oct. 1966, pp. 176–189.

[17] Zel'dovich, Y. and Raizer, Y., *Physics of Shock Waves and High Temperature Hydrodynamic Phenomena*, Vol. II, Academic Press, New York, 1967.

[18] Marshak, R. E., "Effect of Radiation on Shock Wave Behavior," *The Physics of Fluids*, Vol. 1, No. 1, 1958, pp. 24–28.

AUGUST 1970 AIAA JOURNAL VOL. 8, NO. 8

Criteria for Selecting Curves for Fitting to Data

T. J. Dylewski*

Lockheed Missiles & Space Company, Sunnyvale, Calif.

The purpose of curve-fitting is the prediction of future data; thus, criteria should discriminate strongly in favor of curves having high predictive merit for a given phenomenon. If the laws of nature pertaining to a phenomenon are known, they should form the basis for choosing the curve to be fitted. Otherwise, bias is almost sure to exist in the representation of data by an arbitrary curve. Bias is a systematic discrepancy between the fitted curve and the true equation governing the data. Bias can arise from either oversmoothing or undersmoothing. A criterion has been developed which selects a curve of minimum bias for improving the predictability of future data even if the true equation is unknown. The minimum-bias criterion accepts that type of curve for which the ratio of over-all sum of squares of deviations to subset sum of squares of deviations is a minimum.

I. Purpose and Nature of Curve-Fitting

THE purpose of curve-fitting is assumed to be the summarizing of experimental evidence for making predictions with regard to future data. Although this purpose has been clearly stated in the past,[1,2] the literature of the subject reveals little evidence of the explicit use of predictive ability as a criterion of curve-fitting.

The two kinds of prediction possible through curve-fitting, in order of rapidly decreasing accuracy, are 1) interpolation, or prediction of the dependent variable within the range of observed values of the independent variable and 2) extrapolation, or prediction of the dependent variable beyond the range of observed values of the independent variable.

Of course, all predictions at best have only a formal, *ceteris-paribus* validity; that is, all conditions, deterministic as well as probabilistic, must prevail in the future.

Two distinct but interdependent steps in the curve-fitting process determine how well its predictive purpose is realized. These steps are 1) selection of the type of curve to be fitted and 2) evaluation of the constants of the curve.

The two steps are mutually complementary since each satisfies requirements that the other is unable to fulfill. Both must always be done with care. If one is slighted, no amount of meticulous attention to the other can compensate for the neglect. Moreover, execution of these steps should be preceded by a critical review of the data for the purpose of determining whether a curve fitted to them can serve the intended use.

Regardless of the functional relation that it represents, a curve fitted to data can be thought of as simple or complicated, depending on the number of constants that must be evaluated for defining it. The greater the number of constants, the more closely will the curve follow the experimental data. The suitability of a particular curve, however, is always dependent upon the amount of real random fluctuation present in the data.

If the selected curve is too simple, there will be large deviations between the curve and the data; consequently, excellent data may look bad. Conversely, if the curve is too complicated, it will follow closely not only the true variation of the data, but the random fluctuation as well, producing thereby a false impression of high accuracy.

Figures 1 and 2 illustrate how an arbitrary choice of the type of curve in place of the proper one of Fig. 3 can misrepresent the data through either oversmoothing or undersmoothing. Oversmoothing means that some deterministic variation has been regarded as random variation and discarded. Undersmoothing means that some random variation has been regarded as deterministic and has been retained.

It is unfortunate that the phrase "best fit" is commonly used to describe various functional approximations without adequate attention to the criteria upon which the so-called best fit is based. Perhaps the most insidious is the Tschebycheff method of fitting polynomials, which is superficially

Received September 4, 1969; presented as Paper 69–950 at the AIAA Aerospace Computer System Conference, Los Angeles, Calif., September 8–10, 1969; revision received February 2, 1970. The author is grateful to D. Colvin for programing the bias criterion test cases for the Univac 1108 computer and SC 4020 plotter.

* Senior Staff Scientist, Scientific Computing Division. Member AIAA.